Journal of Applied Sciences

ISSN 1812-5654

science alert

ANSInet
an open access publisher
http://ansinet.com

Journal of Applied Sciences 12 (14): 1481-1487, 2012
ISSN 1812-5654 / DOI: 10.3923/jas.2012.1481.1487

Influence of Nanoclay/Phenol Formaldehyde Resin on Wood Polymer Nanocomposites

Md. Rezaur Rahman, Sinin Hamdan, Md. Saiful Islam and Abu Saleh Ahmed
Faculty of Engineering, Universiti Malaysia Sarawak,
94300 Kota Samarahan, Sarawak, Malaysia

Abstract: Selected tropical wood specie was low dense soft wood and it is abundantly available in Borneo Island. This specie is not suitable for construction materials due to their law physical and mechanical properties. In order to overcome this problem the wood species were impregnate by Nanoclay/PF resin system. Raw wood specimens were then placed into an impregnation chamber, in which there was no contact between samples and they were covered completely by nanoclay/PF mixtures. The system was evacuated to 60 mmHg for 30 min. After that, compressed air was applied to the system and maintained at a pressure of 0.52 MPa for 30 min then released. The excess chemicals wiped off the samples. FT-IR spectra indicate the decrease wave number of the peak, ascribed to C-O stretch of C-O-H in starch at 1317 cm^{-1} and 1222 cm^{-1} and C-O stretch of C-O-C in starch at 1027 cm^{-1} confirmed the impregnation of nanoclay/PF wood sample due to the fact that plasticizer could form intense H-bonding interaction with the hydroxyl groups. The MOE and MOR of WPNC were significantly increased compared with raw wood. The Young's modulus of *Eugenia* sp. was significantly different between raw wood and WPNC. The XRD patterns of WPNC indicate that the crystallinity increases at the amorphous region due the monomer loading. The SEM micrograph of WPNC clearly shows the void space was filled by the monomer and removes the waxy substance.

Key words: Modulus of elasticity, modulus of rupture, scanning electron microscopy analysis, X-ray diffraction analysis

INTRODUCTION

Organic or inorganic fillers have been used as reinforcements in polymers. The up to date nanoparticles has attracted much attention in manufacturing polymeric nanocomposites using various nanoparticles as reinforcements. The polymeric nanocomposites showed their different properties based on the experimental results. Some researcher found the improvement of the matrix properties (Lee *et al*., 2011; Hamzah *et al*., 2010; Ratnasingam and Ioras, 2010; Ramasamy and Ratnasingam, 2010; Adebhar *et al*., 2001; Yasmin *et al*., 2003; Kinloch *et al*., 2003) while others reported unfavorable effect (Haggenmueller *et al*., 2006; Zilg *et al*., 1999, 2000) due to the additions of nanoparticles. Moreover, the effect of nanofillers is established its necessity because of its unique properties and reliable method of dispersing nanoparticles is still lacking.

In order to overcome this problem nanoparticles break these bunches and established the shear mixing methods. (Nazerian *et al*., 2011a; H'ng *et al*., 2011; Yasmin *et al*., 2003), mechanical mixing (Shah and Paul, 2004), *in situ* polymerization (Haggenmueller *et al*., 2006; Nazerian *et al*., 2011b; Farrokhpayam *et al*., 2010; Ratnasingam *et al*., 2010a, b) and impregnation have been used to produce nanocomposites. Researchers have been reporting improved mechanical properties of nanocomposites fabricated via the impregnated method. However, with few exceptions, the properties of the resulting nanocomposites tend to go down after reaching the maximum at a particle loading of about 3-5 wt.% or less (Rodgers *et al*., 2005; Choi *et al*., 2005; Zheng *et al*., 2005).

Some articles have been published on silica/epoxy nanocomposites fabricated from organosilicasol (colloidal silica in organic solvent) (Adebhar *et al*., 2001; Kinloch *et al*., 2003; Uddin and Sun, 2008). Uddin and Sun (2008) obtained 40% improvement in matrix compressive modulus with 15 wt.% silica nanoparticle loading. By using this nanoparticle-enhanced matrix, glass fiber composites gained 60-80% in longitudinal compressive strength for different fiber volume fractions. Kinloch *et al*. (2003) reported the greatly improved fracture behavior of an epoxy adhesive with the inclusion of both silica nanoparticles and rubber composites. In this study Nanoclay/Phenol Formaldehyde resin system were used as a reinforcement matrix to produce the WPNC.

Corresponding Author: Md. Rezaur Rahman, Faculty of Engineering, Universiti Malaysia Sarawak,
94300 Kota Samarahan, Sarawak, Malaysia Tel: +6082 583317 Fax: +6082 583410

MATERIALS AND METHODS

Materials: The softwoods *Eugenia* sp., *Artocarpus rigidus*, *Artocarpus elasticus* and *Xylopia* sp. and the hardwood *Koompassia malaccensis* were used for this study since June 2011 to end of December 2011. Chemicals used to impregnate these wood species were Nanoclays nanomer® 1.30E, Montmorillonite (MMT) (Southern Clay Products, Inc. USA) and Phenol Formaldehyde resin (PF) (Merck, Germany). The purity grade of the chemicals were 99%.

Preparation of impregnation solutions: The impregnation solutions were prepared by adding 1% layered aluminosilicate nanofiller into the low viscosity phenol formaldehyde resin at a mixing speed of 2050 rpm for 20 min then nanoclays were mixed with the PF resin prepolymer to form impregnation solutions that were subsequently used to impregnate the wood species.

Manufacturing of wood polymer nanocomposites: Raw wood specimens were oven dried to constant weight at 103°C for 24 h. They were then placed into an impregnation chamber, in which there was no contact between samples and they were covered completely by nanoclay/PF mixtures. The system was evacuated to 60 mm Hg for 30 min. After that, compressed air was applied to the system and maintained at a pressure of 0.52 MPa for 30 min then released. The excess chemicals were wiped off the samples. Specimens were weighted and dried 24 h by air circulation, followed by oven drying at 90°C for 24 h. The excess polymers were then removed from the surface.

FT-IR spectroscopy analysis: The infrared spectra of the raw woods and WPC were recorded on a Shimadzu Fourier Transform Infrared Spectroscopy (FTIR) 81001 Spectrophotometer. The transmittance range of the scan was 370 to 4000 cm^{-1}.

The free- free flexural vibration testing: Determination of the dynamic Young's modulus (E_d) was carried out using the free-free flexural vibration testing system. The specimen was held with AA thread according to the first mode of vibration. The specimen with an iron plate bonded at one end was set facing the electromagnet driver and a microphone was placed at the centre below the specimen. The frequency was varied in order to achieve a resonant or natural frequency. The E_d was calculated from the resonant frequency by using the following equation:

$$Ed = \frac{4\pi^2 f^2 l^4 A\rho}{I (m_n)^4}$$

where, I is $bd^3/12$, d is beam depth, b is beam width, l is beam length, f is natural frequency of the specimen, ρ is density, A is cross sectional area and n = 1 is the first mode of vibration, where $m_1 = 4.730$.

Determination of static Young's modulus (E_s), modulus of elasticity (MOE) and modulus of rupture (MOR): Determination of E_s, MOE and MOR was carried out according to ASTM D-143 (2006). A Shimadzu Universal Testing Machine having a loading capacity of 300 kN was used for the test with the cross head speed of 2 mm/min. E_s was measured using the uniaxial compression test. The MOE and MOR were measured using the three point bending method and were calculated using the following equations, respectively:

$$MOE = \frac{L^3 m}{4bd^3} \quad (1)$$

$$MOR = \frac{1.5PL}{bh^2} \quad (2)$$

Where:

L = Span length of sample, 180 mm
b = Width of sample, 20 mm
d = Thickness of sample, 20 mm
m = Slope of the tangent to the initial line of the force displacement curve
P = The maximum breaking load
h = Depth of the beam

Scanning electron microscopy analysis (SEM): The specimens were first fixed with Karnovsky's fixative and then taken through a graded alcohol dehydration series. Once dehydrated, the specimen was coated with a thin layer of gold before being viewed on the Scanning Electron Microscope (JSM-6701F) supplied by JEOL Company Limited, Japan. The micrographs, taken at a magnification of 150X.

X-ray diffraction analysis (XRD): XRD analysis for raw wood and Wood Polymer Composites (WPC) were performed with a Rigaku diffractometer (CuK α radiation, λ = 0.1546 nm) running at 40 kV and 30 mA.

RESULTS AND DISCUSSION

Fourier transforms infrared (FTIR) spectroscopy analysis: FTIR spectra of raw wood and WPNC are shown in Fig. 1. The spectra were separated in two regions, namely: the OH stretching vibrations in 4000-2700 cm^{-1} region and fingerprint region in 1800-400 cm^{-1}

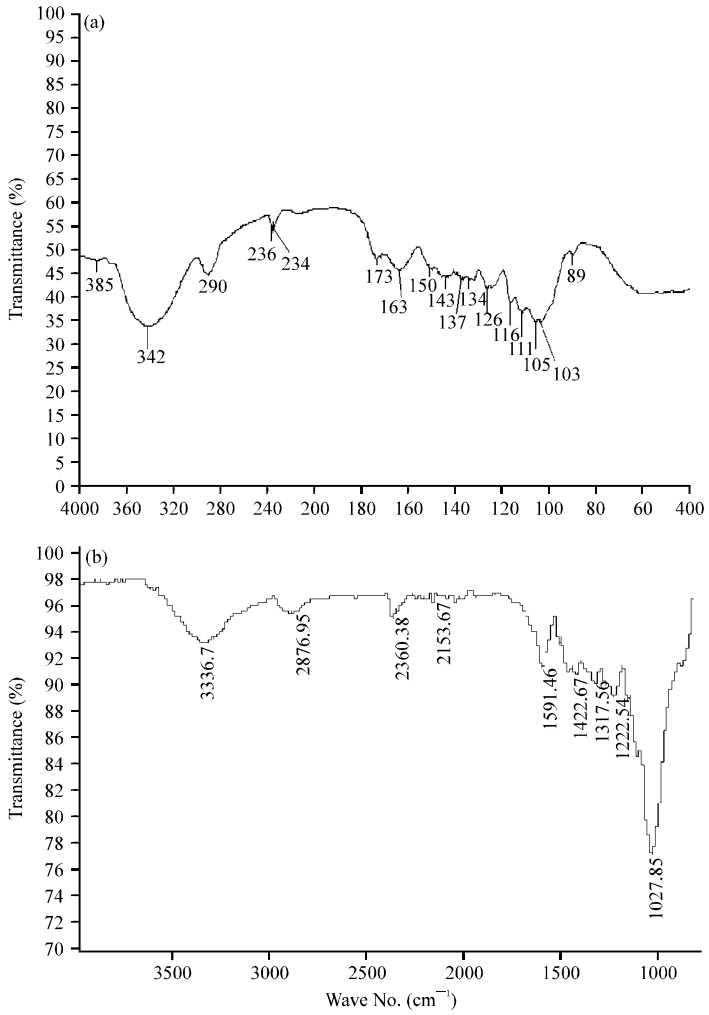

Fig. 1(a-b): IR spectrum of (a) Raw wood and (b) WPNC

region. The stretching band of OH group and C-H group was 3300-4000 cm^{-1} and 2800- 3000 cm^{-1}, respectively. The band region from 1000 to 1750 cm^{-1} shown the superposition with sharp and discrete absorptions (Owen and Thomas, 1989). The absorption band 1508 cm^{-1} is caused by lignin and the absorption located at 1735 cm^{-1} is caused by hemicelluloses. This indicates the C = O stretch in non-conjugated ketones, carbonyls and ester groups (Owen and Thomas, 1989). The region between 1800 and 1100 cm^{-1} comprises bands assigned to the main components from wood: cellulose, hemicelluloses and lignin. Clear difference can be detected in the infrared spectra, both in the different absorbance values and shapes of the bands and their location. The less xylan content in softwood is evidenced by a carbonyl band at 1735 cm^{-1}, for nanoclay/PF modified wood, this being shifted to a lower wave number value (1591 cm^{-1}). On the other hand, the decrease wave number of the peak, ascribed to C-O stretch of C-O-H in starch at 1317 and 1222 cm^{-1} and C-O stretch of C-O-C in starch at 1027 cm^{-1} confirmed the impregnation of nanoclay/PF wood sample due to the fact that plasticizer could form intense H-bonding interaction with the hydroxyl groups.

Dynamic Young's modulus measurement: The dynamic Young's modulus of the raw wood and WPNC, from the free-free flexural vibration testing system is shown in Fig. 2. Ten specimens were used for each species. The nanofiller with phenol formaldehyde monomer system increased the Young's modulus, as seen in all species which was according to our previous work (Hamdan *et al*., 2010). After monomer impregnation the Young's modulus of *Eugenia* sp., *Xylopia* sp., *Artocarpus rigidus* and *Artocarpus elasticus*, were significantly higher than that of raw one. On the other hand the Young's modulus of *Koompassia malaccensis* was slightly higher due to their hard cell wall (due to the nanofiller effect on all wood species).

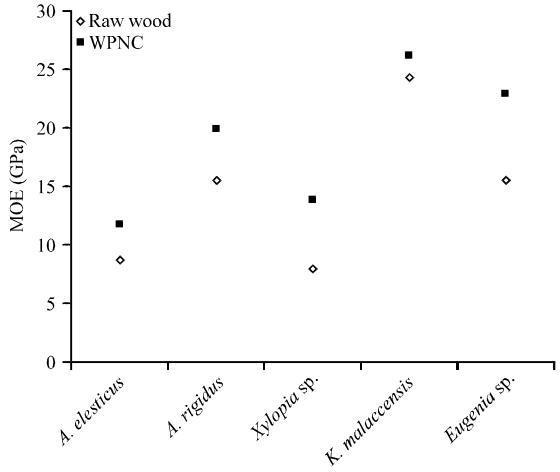

Fig. 2: Dynamic Young's modulus of raw wood, WPNC for all species

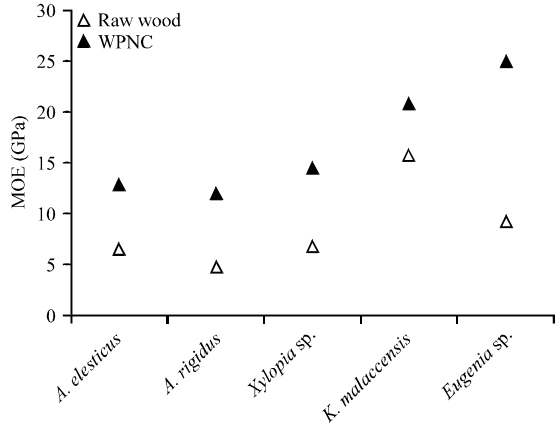

Fig. 3: MOE of raw wood and WPNC

Modulus of Elasticity (MOE) and modulus of rupture (MOR) measurement: The MOE and MOR of raw wood and WPNC are shown in Fig. 3 and 4, respectively. The nanofiller phenol formaldehyde monomer system impregnation on the discerning wood species was investigated. The increment in MOE of the *Eugenia* sp. and *Xylopia* sp. were highest followed by, *Artocarpus rigidus, Artocarpus elasticus* and *Koompassia malaccensis*, respectively. WPNC yielded higher MOE compared to the raw wood because of the impact of nanofiller on wood species which is in accordance with other researchers (Cai *et al*., 2007, 2008).

From Fig. 3, the MOE of the *Eugenia* sp., *Xylopia* sp., *Artocarpus elasticus* and *Artocarpus rigidus* were significantly higher compared with raw wood. However in *Koompassia malaccensis*, (hardwood) there was no significant effect of nanomer impregnation but increment in MOE was slightly higher than that of our previous work.

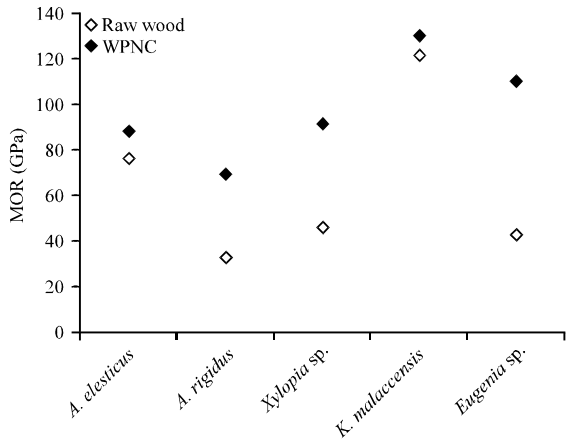

Fig. 4: MOR of raw wood and WPNC

In the wood specimens, phenol formaldehyde plasticizes on the cellulose and hemicellulose in wood cells which reduces the water molecules from the wood specimens. During the nanoclay phenol formaldehyde monomer impregnation nanofiller react as a binder which fill the void space in the wood specimens and increase it stiffness. For this reason the MOE of all WPNC was higher than that of raw wood (Fig. 3).

The MOR of *Eugenia* sp. WPNC was radically increased after nanofiller with phenol formaldehyde impregnation. The MOR also improved after nanofiller/phenol formaldehyde impregnation in accordance with previous research (Cai *et al*., 2007, 2008).

Figure 4 indicates that the MOR was significantly different for *Xylopia* sp., *Artocarpus rigidus, Artocarpus elasticus and Eugenia* sp. raw wood and WPC. The growth of MOR for *Eugenia* sp. was highest followed by *Xylopia* sp., *Artocarpus rigidus, Artocarpus elasticus* and *Koompassia malaccensis*, respectively. The value for *Koompassia malaccensis* (hardwood) WPNC was higher than that of raw one.

Static Young's modulus (E_s) measurement: The Static Young's modulus was determined from 10 repetitions, as summarized in Fig. 5. The highest increment of E_s value was observed in *Eugenia* sp. followed by *Artocarpus rigidus, Artocarpus elasticus, Xylopia* sp. and *Koompassia malaccensis*, respectively. Figure 5 indicates that, the increment of E_s between raw wood and WPNC for *Eugenia* sp. was significantly different. The increment of E_s in WPNC compared to raw wood was also reported by different researchers (Cai *et al*., 2007, 2008; Rahman *et al*., 2010). The nanofiller/phenol formaldehyde not only plasticized on the wood cell walls but also deeply increasing their lateral stability.

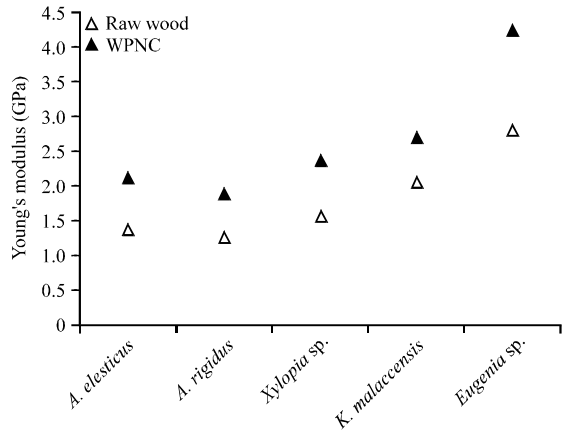

Fig. 5: Static Young's modulus of raw wood and WPNC

XRD analysis: Figure 6 presents the results of XRD for raw wood and WPNC. The spectrum corresponding to the raw wood and WPNC shows diffraction peaks at the following 2θ angles: 17°, 22.5° and 35° which correspond to the cellulose crystallographic planes 101, 002 and 040, respectively (Mulinari *et al*., 2010). The position of these peaks did not change which indicates that the structure of cellulose did not change in comparison with the raw wood. It is observed that the WPNC exhibited another five broad 2θ peaks at 43.74°, 49.21°, 51.13°, 55.65° and 72.87° which are due to increasing polymerization in the amorphous region.

These values can be attributed to modification of the wood by the nanofiller/phenol-formaldehyde prepolymer. The reason may be that the prepolymer has been injected into the lumen of wood cell. The crosslinking reaction occurred between the groups of prepolymer and the surface hydroxyl (OH) groups of wood. A quasi-crystalline form was generated in the XRD, but actually it may not represent an increase in the crystallinity of cellulose (Wu *et al*., 2004).

Scanning electron microscopy (SEM) analysis: Scanning Electron Micrographs (SEM) of raw wood and WPNC are shown in Fig. 7. The SEM micrographs showed that the raw wood surfaces were covered with an uneven layer with a number of void/hole spaces, while the treated wood surfaces were smooth (Fig. 7a, b). The smooth surface may be caused by the good penetration of the monomer mixture to the cell wall and vessels of the wood (Rahman *et al*., 2010). The SEM analysis indicated that the prepolymer was impregnated into cell wall and cell cavities of wood.

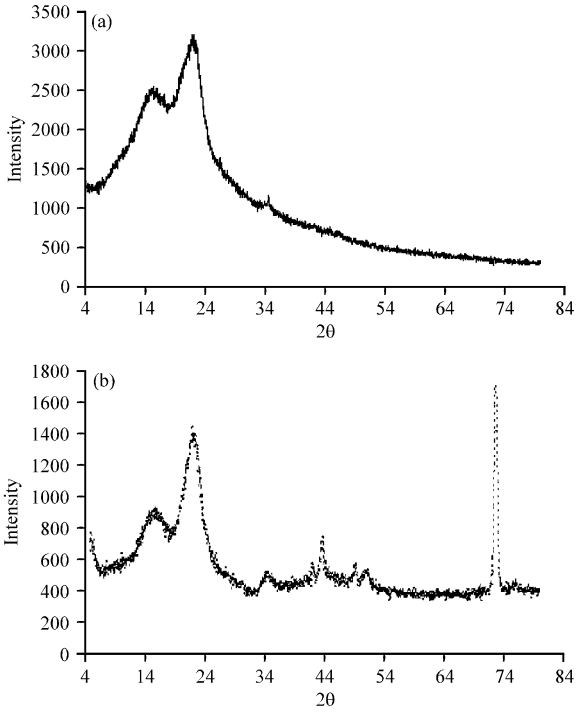

Fig. 6(a-b): X-ray diffraction of (a) Raw wood and (b) WPNC

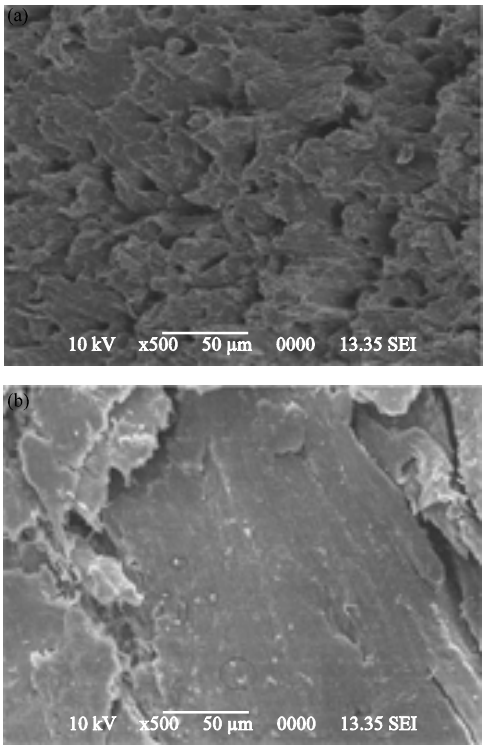

Fig. 7(a-b): Scanning electron microscopy of (a) Raw wood and (b) WPNC

CONCLUSION

In the present study nanofiller/phenol formaldehyde WPC were investigated. FT-IR spectra indicate the decrease wave number of the peak, ascribed to C-O stretch of C-O-H in starch at 1317 cm^{-1} and 1222 cm^{-1} and C-O stretch of C-O-C in starch at 1027 cm^{-1} confirmed the impregnation of nanoclay/PF wood sample due to the fact that plasticizer could form intense H-bonding interaction with the hydroxyl groups. The stiffness of the WPNC was significantly increased compared with raw wood. The MOE and MOR of WPNC were significantly increased for *Eugenia* sp., *Xylopia* sp., *Artocarpus Rigidus* and *Artocarpus Elasticus* respectively. The Young's modulus of *Eugenia* sp. was significantly different between raw wood and WPNC. The XRD patterns of WPNC indicate that the crystallinity increases at the amorphous region due the monomer loading. The SEM micrograph of WPNC clearly shows the void space was filled by the monomer and removes the waxy substance. It can be concluded that nanofiller/phenol formaldehyde was significantly effective on *Eugenia* sp. followed by *Xylopia* sp., *Artocarpus Rigidus* and *Artocarpus Elasticus* wood species, respectively.

REFERENCES

ASTM D-143, 2006. Standard method of testing small clear specimens of timber. American Society for Testing and Materials, USA.

Adebhar, T., C. Roscher and J. Adam, 2001. Reinforcing nanoparticles in reactive resins. Eur. Coat J., 4: 144-149.

Cai, X., B. Riedl, S.Y. Zhang and H. Wan, 2007. Formation and properties of nanocomposites made up from solid aspen wood, melamine-urea-formaldehyde and clay. Holzforschung, 61: 148-154.

Cai, X., B. Riedl, S.Y. Zhang and H. Wan, 2008. The impact of the nature of nanofillers on the performance of wood polymer nanocomposites. Applied Sci. Manuf., 39: 727-737.

Choi, Y.K., K.I. Sugimoto, S.M. Song, Y. Gotoh, Y. Ohkoshi and M. Endo, 2005. Mechanical and physical properties of epoxy composites reinforced by vapor grown carbon nanofibers. Carbon, 43: 2199-2208.

Farrokhpayam, S.R., J. Ratnasingam, E.S. Bakar and S.H. Tang, 2010. Characterizing surface defects of solid wood of dark red meranti (*Shorea* sp.), melunak (*Pentace* sp.) and rubberwood (*Hevea brasiliensis*) in planing process. J. Applied Sci., 10: 915-918.

H'ng, P.S., A.N. Lee, C.M. Hang, S.H. Lee, A. Khalina and M.T. Paridah, 2011. Biological durability of injection moulded wood plastic composite boards. J. Applied Sci., 11: 384-388.

Haggenmueller, R., F. Du., J.E. Fischer and K.I. Winey, 2006. Interfacial in situ polymerization of single wall carbon nanotube/nylon 6,6 nanocomposites. Polymer, 47: 2381-2388.

Hamdan, S., Z.A. Talib, M.R. Rahman, A.S. Ahmed and M.S. Islam, 2010. Dynamic Young's modulus measurement of treated and post-treated tropical Wood Polymer Composites (WPC). Bioresources, 5: 324-342.

Hamzah, M.O., A. Jamshidi, Z. Shahadan, M.R.M. Hasan and A.S. Yahaya, 2010. Evaluation of engineering properties and economic advantages of WMA using local materials. J. Applied Sci., 10: 2433-2439.

Kinloch, A.J., J.H. Lee, A.C. Taylor, S. Sprenger, C. Eger and D. Egan, 2003. Toughening structural adhesives via nano-and micro-phase inclusions. J. Adhes, 79: 867-873.

Lee, S.H., P.S. H'ng, M.J. Chow, A.S. Sajap, B.T. Tey, U. Salmiah and Y.L. Sun, 2011. Effectiveness of pyroligneous acids from vapour released in charcoal industry against biodegradable agent under laboratory condition. J. Applied Sci., 11: 3848-3853.

Mulinari, D.R., H.J.C. Voorwald, M.O.H. Cioffi, G.J. Rocha and M.L.C.P. Da Silva, 2010. Surface modification of sugarcane bagasse cellulose and its effect on mechanical and water absorption properties of sugarcane bagasse cellulose/HDPE composites. BioResources, 5: 661-671.

Nazerian, M., E. Gozali and M.D. Ghalehno, 2011a. The influence of wood extractives and additives on the hydration kinetics of cement paste and cement-bonded particleboard. J. Appl. Sci., 11: 2186-2192.

Nazerian, M., M.D. Ghalehno and A.B. Kashkooli, 2011b. Effect of wood species, amount of juvenile wood and heat treatment on mechanical and physical properties of laminated veneer lumber. J. Applied Sci., 11: 980-987.

Owen, N.L. and D.W. Thomas, 1989. Infrared studies of hard and soft woods. Applied Spectrosc., 43: 451-455.

Rahman, M.R., S. Hamdan, A.A. Saleh and M.S. Islam, 2010. Mechanical and biological performance of sodium mataperiodate impregnated Plasticized Wood (PW). BioResources, 5: 1022-1035.

Ramasamy, G. and J. Ratnasingam, 2010. A review of cemented tungsten carbide tool wear during wood cutting processes. J. Applied Sci., 10: 2799-2804.

Ratnasingam, J. and F. Ioras, 2010. Static and fatigue strength of oil palm wood used in furniture. J. Applied Sci., 10: 986-990.

Ratnasingam, J., F. Ioras and T. McNulty, 2010a. Fatigue strength of mortise and tenon furniture joints made from oil palm lumber and some Malaysian timbers. J. Applied Sci., 10: 2869-2874.

Ratnasingam, J., T.P. Ma and G. Ramasamy, 2010b. Tool temperature and cutting forces during the machining of particleboard and solid wood. J. Applied Sci., 10: 2881-2886.

Rodgers, R.M., H. Mahfuz, V.K. Rangari, N. Chisholm and S. Jeelani, 2005. Infusion of SiC nanoparticles into SC-15 epoxy: An investigation of thermal and mechanical response. Macromol. Mater. Eng., 290: 423-449.

Shah, R.K. and D.R. Paul, 2004. Nylon 6 nanocomposites prepared by a melt mixing masterbatch process. Polymer, 45: 2991-3000.

Uddin, M.F. and C.T. Sun, 2008. Strength of unidirectional glass/epoxy composite with silica nanoparticle-enhanced matrix. Compos. Sci. Technol., 68: 1637-1643.

Wu, C.L., X.P. Li and S.L. Qing, 2004. Cellulose solvent: Current research status and its application prospect. Trans. China Pulp Paper, 19: 171-175.

Yasmin, A., J.L. Abot and I.M. Daniel, 2003. Processing of clay/epoxy nanocomposites by shear mixing. Scripta Mater., 49: 81-86.

Zheng, Y., R. Ning and Y. Zheng, 2005. Study of SiO_2 nanoparticles on the improved performance of epoxy and fiber composites. J. Reinf. Plastic Compos., 24: 223-233.

Zilg, C., R. Mulhaupt and J. Finter, 1999. Morphology and toughness/stiffness balance of nanocomposites based upon anhydride-cured epoxy resins and layered silicates. Macromol. Chem. Phys., 200: 661-670.

Zilg, C., R. Thomann, J. Finter and R. Mulhaupt, 2000. The influence of silicate modification and compatibilizers on mechanical properties and morphology of anhydride-cured epoxy nanocomposites. Macromol. Mater. Eng., 280-281: 41-46.